Generation and evaluation of a synthetic dataset to improve fault detection in district heating and cooling systems

Mathieu Vallee, Thibaut Wissocq, Yacine Gaoua, Nicolas Lamaison

Generation and Evaluation of a Synthetic Dataset to improve Fault Detection in District Heating and Cooling Systems

Mathieu Vallee [a], Thibaut Wissocq [a], Yacine Gaoua [a], Nicolas Lamaison [a]

[a] Univ. Grenoble Alpes, CEA, LITEN, DTCH, LSET, F-38000 Grenoble, France

Abstract:

This paper investigates various types of faults in District Heating & Cooling (DHC) systems. Many authors point out that the lack of data hinders the development of good data-driven models for fault detection and diagnosis (FDD). In this work, we design a reference dataset based on simulation and use it to evaluate Machine Learning (ML) models for fault detection.

The dataset itself covers six types of DHC system components, covering production, distribution and storage. It is provided as Open Data with corresponding documentation. Most of the models used for generating the dataset are provided as Open Source code.

To assess the usefulness of the dataset, we evaluated five ML models on five fault detection tasks. The results highlight varying level of performance on the considered tasks, with faults related to global energy efficiency being easier to handle than those related specifically to thermal losses. Three of the investigated models (Logistic Regression, Support Vector Machine, and XGBoost) provide consistent performance on the considered tasks, achieving accuracy scores up to 99% on the easier tasks and above 66% on one of the more difficult tasks. We also illustrate possibilities for transferring models to real systems with different characteristics, with encouraging results.

Keywords:

District Heating and Cooling, Synthetic Dataset, Fault Detection and Diagnosis, Machine Learning

Abbreviations:

DHC	District Heating and Cooling
FDD	Fault Detection and Diagnosis
ML	Machine Learning
FMECA	Failure Mode, Effect and Criticality Analysis
TRL	Technology Readiness Level
IEA	International Energy Agency
BES	Building Energy System
HVAC	Heating, Ventilation and Air-Conditioning
EBC	Energy in Buildings and Communities
CHP	Combined Heat and Power
HEX	Heat EXchanger
SST	SubSTation
LMTD	Logarithmic Mean Temperature Difference
COP	Coefficient Of Performance

1 INTRODUCTION

1.1 Background on District Heating&Cooling Systems, Digitalization and Fault Detection

The development of District Heating & Cooling (DHC) Systems is becoming a cornerstone of many European country policies for decarbonization, especially since the Green Deal. This type of system, as any technical processes, is subject to dysfunctions during their lifespan. The development of robust fault detection and diagnosis (FDD) methods is therefore a key issue to boost efficiency.

Digitalisation and the increasing availability of data from various sensors can provide new opportunities for FDD. Even if this trend is still not so widespread in DHC compared to other fields, efforts in this direction have been scaling up in recent years [1], [2]. Several recent reviews recognize the opportunities for Machine-Learning in DHC systems, however applications of this approach for FDD are still limited [3], [4].

1.2 Overview of current FDD approaches

FDD approaches are often decomposed into three broad categories, as illustrated by Figure 1. Both the quantitative and qualitative model-based approaches rely heavily on models produced by experts. Process-history based approaches, nowadays rather referred to as “data-driven approaches”, rely on data collected from the systems, and automatic methods for building models from this data.

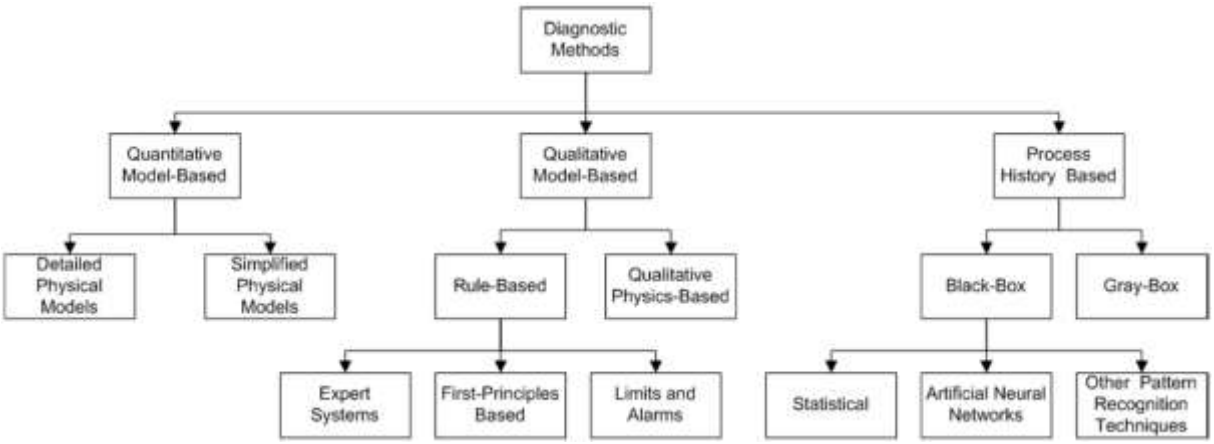

Figure 1 - Classical classification scheme for FDD methods. ([5], adapted from [6], also adapted in [7]–[9], among others)

Both model-based and data-driven approaches have their advantages and limitations, as summarized for instance by [10]. In particular, setting up dedicated physical simulation models may require a significant effort, while data-driven model require data in sufficient quantity and quality to be useful. To alleviate these limitations, hybrid methods can be investigated. The possibility to consider various mixes of modeling expertise and data (from white-box to black-box models) was already pointed out by Rolf Isermann in his reference book on FDD ([11], see section 5.2.1 and figure 5.10). However, recent progress in machine learning methods make it more and more feasible to rely on purely black box models, if enough meaningful data is available.

1.3 Previous work on FDD applicable to DHC systems

In this work, we investigate solutions for DHC system operators to detect and diagnose faults at system level. The authors conducted a detailed analysis on typical faults in DHC systems in the context of the IEA DHC Annex XIII [12]. This analysis highlights a number of faults on various components of a DHC system which would be relevant for monitoring at DHC system level using the data already available from usual process monitoring. Other types of faults are: (1) faults located directly on sensor or actuators, (2) faults which are already present at commissioning, (3) faults which are correctly detected by existing solutions**.** For sensor and actuator faults, generic methods can be designed based on operational data, as for instance in [13]. Previous works addressing the other two types of fault typically require additional or external measurements dedicated to FDD (e.g. infrared thermography), or sensors on particular components (e.g. pump [9] or gas turbine [14]) which could be available in newer equipment but would be hard to retrofit on existing equipment. They are not investigated further in the following.

When considering production components in a DHC system, FDD has been investigated by previous work not only in the DHC context but also in similar set-ups at building level or industrial plants. For typical boilers and CHP, Panday et al.[15] provides a recent state of the art of fault locations and detection methods. Hundi and Shavari [16] study global faults leading to a lack of efficiency, which is particularly relevant in the DHC system. For heat pump and chillers, most previous work on FDD apply to single buildings, but would be applicable at DHC system level. Most works agree on the set of faults to consider, which was initially identified in [17] (section 3.2). All of these faults do not lead to an immediate stop of the device, and may therefore go unnoticed. Kim et al. provide an analysis of their impact on energy efficiency [18]. Although many works in the literature concentrate on air-to-air chillers, the described faults also apply to water-to-water machines used in DHC systems. In particular, relevant FDD approaches are in development for HVAC in BES [19]–[23]

Regarding the pipe network, we can distinguish three types of faults affecting the distribution network itself: leaks, insulation faults (thermal losses), and hydraulic distribution faults (insufficient pressure difference, unwanted bypasses, and valves in wrong position). All these types of faults lead to an overall lack of efficiency of the network. Important leaks may also lead to a complete failure of heat distribution in some parts of the network. Recently, several works have been investigating efficient data-driven methods to detect leaks in DHC networks, with the help of simulation [24]–[26].

Regarding substations, a study by Gadd and Werner [27] indicates that a high proportion of faults in DHC system occurs in substations, and considered 3 main types of faults: unsuitable heat load pattern, low average annual temperature difference, poor substation control. Buffa et al. [10] (section 3.2) provide a recent review of work related to fault detection in substations. In particular, they refer to the work of Månsson et al. [28], which provides a detailed taxonomy of faults observed in Swedish substations. In a similar work conducted in Austria, Leoni et al. [29] report that two of the main reported causes for high return temperatures deal with the substation valves and control. Fabre [30] studies malfunctions of substations in a French context, and especially the consequence of fouling and bad regulation. All these works complement the analysis

conducted in the IEA EBC report ([17], section 3.1.2) with more details based on observations in current DHC systems and feedback from DHC operators. Among the list consolidated by previous literature, many of the faults are due to a wrong installation or configuration of the equipment (wrong commissioning). A few others may appear during the operation. In most cases, maintenance teams should be able to detect and diagnose broken actuators, stuck control valves and heat exchanger leakage. However, heat exchanger fouling, incorrect regulation and sensor failures may go unnoticed while degrading the overall performance of the system. With the increasing availability of data from substation monitoring, data-driven detection of fouling has been investigated for instance by [31].

Regarding storage in water tanks, the analysis conducted in the IEA EBC report ([17], section 3.4) indicates that many faults are caused by a wrong interaction between the storage tank and the rest of the system (in their case a heat pump), leading in particular to incorrect temperature levels flowing in or out of the tank. Faure [8] reports similar issues in the context of tank coupled to a solar thermal system. Among the twelve main faults identified in the IEA EBC report ([17], section 3.4), five faults occur at design time. The seven faults occurring in operation are classified into four type of hardware faults (water proofing damage, insulation damage, too high or too low flow in two-way valves), two types of control faults and one sensor fault. For control and sensor faults generic methods can be applied. Other faults seem to remain unaddressed in the available literature.

Many of the work in the literature indicate that the lack of data in sufficient quantity and quality, especially regarding ground truth labelling, hinders the development of good data-driven models ([10], [32], [33], among others). Exploiting simulation models to produce data for machine learning is one of the most prominent trends identified in hybrid Machine Learning methods [34], [35], and is also applied to energy systems modeling and optimization [32], [36], [37]. In the process engineering domain, the open availability of the Tennessee Eastman Process models and simulation data [38], [39] has fostered a number of results on ML and FDD. Novel methods such as transfer learning may also be of interest as it can help adapting a model to a different system than the (simulated) one it was trained on [22], [23].

1.4 Novelty and contribution of this study

In this work, we investigate the possibility for DHC operators to detect and diagnose faults in a DHC system under the following assumptions:

1. We only rely on the data which are typically available for usual monitoring and operation of the DHC system. We assume that no further investment is required in terms of sensors, and that the approach can be deployed only at the cost of a proper collection and archiving of the available data (which may require some investment when it is not in place).
2. The datasets collected by DHC operator do not have to contain previous examples of faults with correct annotation. This aspect is critical for real-world deployment, where annotated datasets are seldom available and would be too costly to create upfront.

In this context, the main contribution of this study is **to design and to evaluate a reference dataset and Machine Learning models for fault detection in a DHC system**. This is expected to improve the FDD capabilities in the DHC field, as well as to trigger new research based on the findings. To ensure reproductibilitiy, we provide not only the dataset as Open Data, but also the models used to generate it and the evaluation of Machine Learning algorithms as Open Source code. Considering the recently proposed Technology Readiness levels for Machine Learning systems [40], we hope this effort will participate to bringing ML technologies for FDD in DHC to TRL level 3 and beyond.

2 MATERIAL AND METHODS

2.1 Overview of the proposed approach

Figure 2 provides an overview of the proposed approach, and indicates how the different stages map to the sections in this paper.

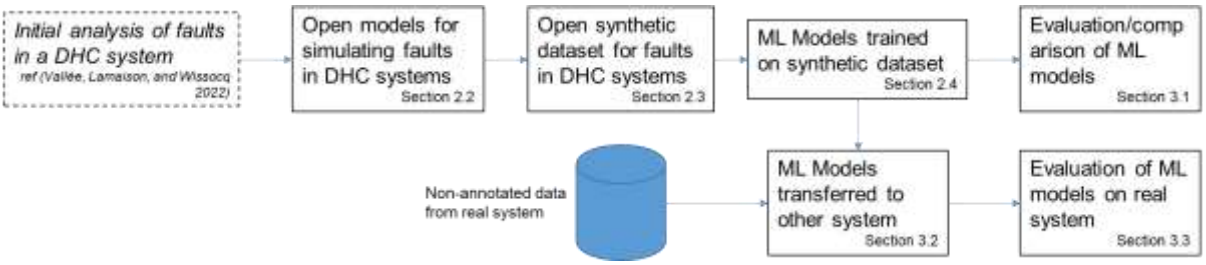

Figure 2 - Overview of the proposed approach

2.2 Generation of the synthetic fault dataset

The methodology for generating fault data from simulation models is derived from previous work conducted by Faure et al [41], as well as similar work in the literature [32].

It can be decomposed into four main steps:

1. Conduct a preliminary analysis, typically a Failure Modes, Effects and Criticality Analysis (FMECA)

2. Define model features required for fault simulation

3. Set up the simulation models

4. Perform simulations to generate diverse fault data

Setp 1 is conducted in [12] and provides a list of faults to simulate.Further steps are described in the following. In order to make the approach reproducible and open, we chose to conduct our analysis based on existing Open Source software libraries. Figure 3 presents the process for identifying and selecting models. In total, we analysed 95 models from 9 Open Source Modelica libraries.

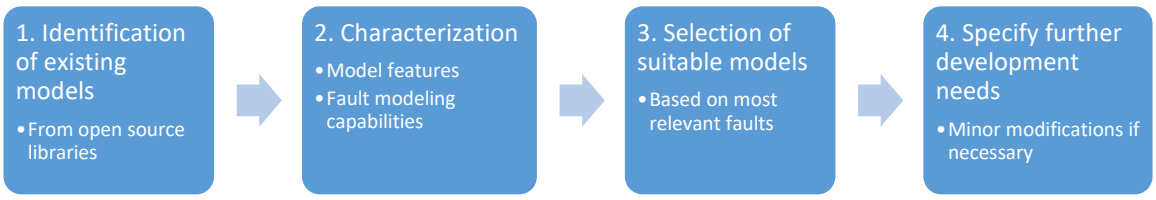

Figure 3 - Process for identifying and selecting fault simulation models

Table 1 provides a synthetic summary of the selected faults and models to simulate them. Details on the model analysis and selection can be found in [12].

Table 1 - Summary of selected faults and Modelica models to simulate them. Underlined models have been used in this work.

Component	Simulated faults	Short list of models (and selected model)
Boiler & CHP	Excessive Heat Loss Low Thermal Efficiency	AixLib/BoilerNoControl, AixLib/CHPNoControl, TransiEnt/SimpleGasBoiler, TransiEnt/DetailedCHP
Heat pump & chiller	COP drop	AixLib/HeatPump, TransiEnt/Heatpump
Solar thermal	Abnormal transmittance values Hydraulic unbalance	CEA/DistrictHeating/SolarThermal (private)
Network (pipe, valves & pump)	Leaks Excessive Heat Loss	DistrictHeating/LinearNetwork (private)
Substations	Heat Exchanger Fouling	DistrictHeating/SubStation (private)
Hot water storage	Excessive heat Loss	IBPSA/Stratified

In most cases, we simulate faults by modifying one or more global parameters of the model (efficiency, thermal losses …). In practice, such modifications could come from various types of faults. Although the finer details of the faults are not modeled here, it is still possible to detect the appearance of an abnormal global behavior, which can then be diagnosed with a further analysis.

For most of the models, the parameters affected by faults were fixed or modifiable only at start time. It was thus necessary to modify them in order to set the fault evolution as an input. In some cases, other modifications were necessary.

To introduce the required diversity in the simulated fault dataset, we defined the models so that different boundary conditions and fault profiles can be applied.

We defined a set of possible boundary conditions suitable for all type of models. These boundary conditions are defined by:

- Weather time series at a time step of 1 hour (extracted from MeteoNorm). They contain the ambient temperature $T_{ext}(t)$, global horizontal solar irradiance $G_{tot}(t)$ and diffuse horizontal solar irradiance $G_{diff}(t)$ for the location of Grenoble (latitude 45.188, longitude 5.724).
- District heating time series, generated from the weather file and generic DH profiles. They contains the heat demand $P_{DHN}(t)$, supply temperature $T_{sup}(t)$, return temperature $T_{ret}(t)$ and mass flow rate $\dot{m}_{flow}(t)$.

Based on a one year weather file, we generated 13 boundary condition profiles, with a duration of four weeks each. It is assumed that this time scale is sufficient for detecting a fault even if it appears progressively.

Different fault apparition profiles are applied and are illustrated in Figure 4. They are defined by the following parameters:

- A profile type which can be either a step or a ramp.
- A start time t_0 at which the fault appears.

- A final time t_f (for the ramp profile only) where the fault gets its final intensity.
- An initial intensity v_0 which is always 0 here.
- A final intensity v_f which is between 0 and 1.

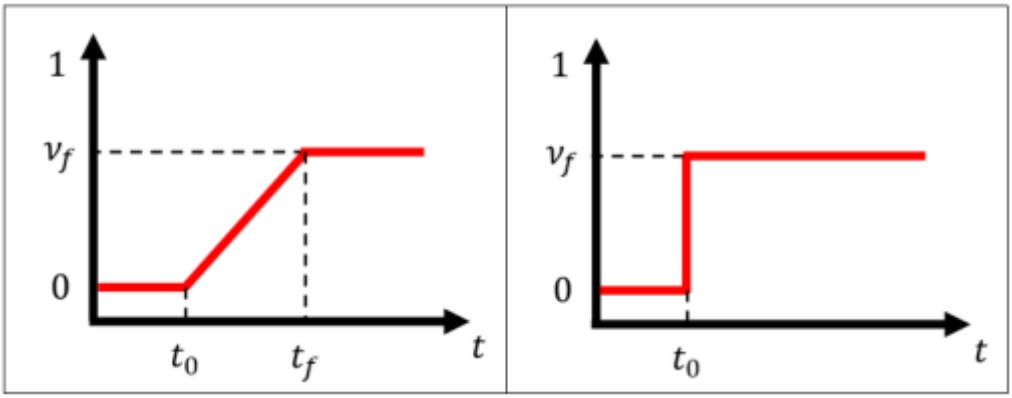

Figure 4 - Fault apparition profiles used in the simulation (left : ramp for progressive faults, right: step for abrupt faults)

The intensity is expressed between 0 and 1, 0 corresponding to no fault and 1 corresponds to the maximal fault intensity available in the model. It depends on model and fault type.

To avoid too much regularity in the results with machine learning algorithm, the fault parameters are set using a random generator. The parameters can also be set manually.

Finally, an example of a fault simulation setup in Modelica is presented in Figure 5. It consists in the simulation of the model *BoilerNoControl* from the AixLib Modelica Library [42], with minor modifications in order to have some variable inputs (efficiency and thermal losses). In this case, the boiler is driven to follow a supply temperature from the boundary conditions. An input file is provided to the model in order to impose a fault signal on efficiency or heat losses after a certain time.

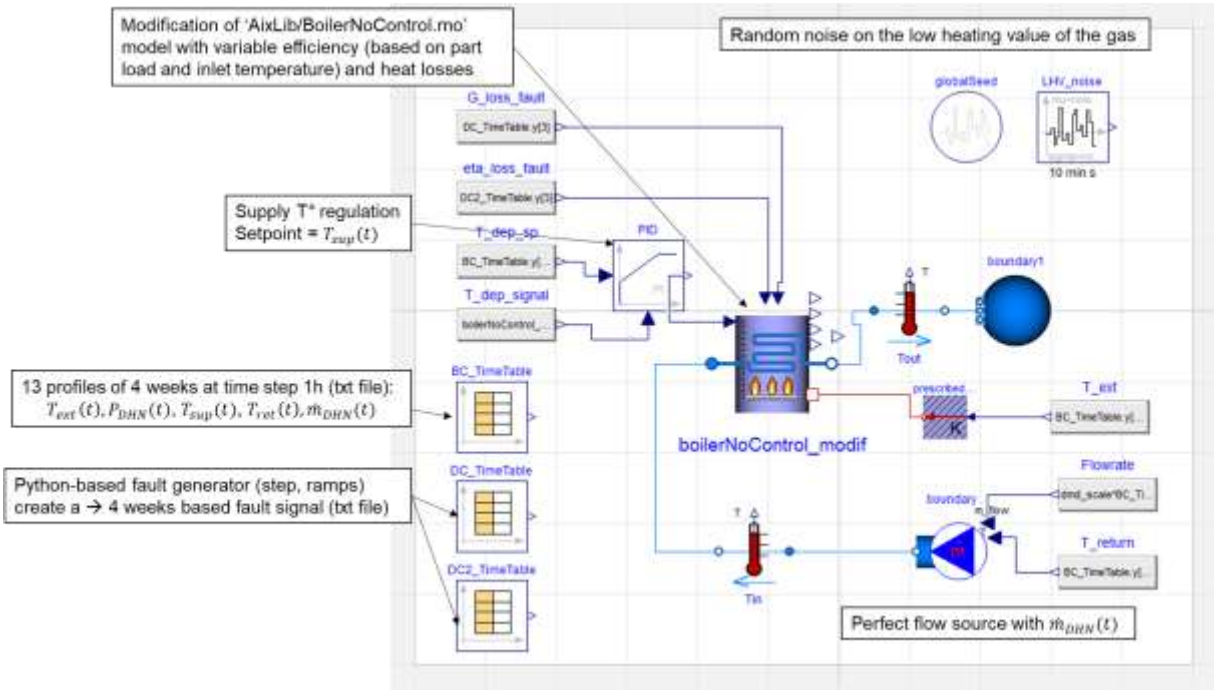

Figure 5 - Fault simulation setup for the boiler case using the model from AixLib.

Details on the other models can be found in [12] and online repository [43].

2.3 Overview of the generated synthetic dataset

Table 2 gives an overview of the dataset we generated and used for this study. We refer the reader to [12] for details on the choice of simulated faults and on the data generation process. For each simulated fault, this table provides:

- The component used in a simulation.
- The fault imposed during a simulation.
- The dataset composition, .i.e., how we defined the simulation experiments that generated this dataset. For instance, the expression "13 x 4 weeks x 10 min x (100 random faults + 1 reference)" means that we used 13 different time series of 4 weeks lengths each, sampled at a 10 minutes frequency, and that we generated 100 simulations with random faults and one reference case with no fault for each boundary conditions setting.
- The total number of records obtained, corresponding to the number of variables times the number of instants recorded in the simulation. It is provided here to give an idea of the total size of the dataset.
- The number of variables in each record, detailed as $N_b + N_x + N_y + N_h$ where:
    - N_b is the number of variables from the boundary conditions. By definition, these variables have the same values for each experiment using a given boundary conditions time series. In practice, there are usually 4 boundary condition variables, which are the external temperature T_{ext} [°C], the heat demand of the network P_{DNH} [kW], the network supply temperature T_{sup} [°C], and the network return temperature T_{ret} [°C]. For solar thermal models, the global horizontal solar irradiance $G_{tot}(t)$ and diffuse horizontal solar irradiance $G_{diff}(t)$ are also included.

- N_x is the number of explicative variables considered as input in fault detection models. These variables are selected from the simulation to represent variables that could effectively be available as sensor measurement in a typical DHC system.
- N_y is the number of target variables. In our case, there is always only 1 target variable, corresponding to the fault status. By convention, the value 0 always denotes a no-fault situation and other possible values depend on the considered fault setup:
  - $y \in \{0,1\}$ denotes a binary classification task. The value 1 denotes the presence of a fault.
  - $y \in \{0,1,2,3\}$ denotes a case with multiple possible faults. It is used for the boiler and CHP component, where we considered two potential faults. The value 1 denotes a efficiency fault, 2 denotes excessive heat losses, 3 denotes both faults at the same time.
  - $y \in \{0 \dots 9\}$ is used for the pipe network case, and denotes the location of the fault (leak or excessive losses). The value denotes the location of the affected piping section (9 sections considered).
  - $y \in \{0 \dots 10\}$ is used for the solar thermal field case, and denotes the location of the faulty column (10 columns considered).
  - $y \in \{0 \dots 5\}$ is used for the solar thermal field case, and denotes the location of the faulty line (5 lines considered).
- N_h is the number of hidden variables. These variables are extracted from the simulation results for visualization and analysis purposes, but are not accessible to machine learning models as they would not be accessible directly in a real DHC system.

In total, the dataset contains about 33 million records, and weight around 2.2 Gb of data (in compressed format). It is provided at [44].

Table 2 - Description of the generated dataset used for machine learning

Component	Simulated faults	Dataset composition	Number of variables (N_b+N_x+N_y+N_h)	Number of records
Boiler & CHP	Low Thermal Efficiency - eta	13 x 4 weeks x 10 min x (100 random faults + 1 reference)	4+3+1+2=10	5.29e6
	Excessive Heat Loss - hls	13 x 4 weeks x 10 min x (100 random faults + 1 reference)	4+3+1+2=10	5.29e6
	Combined eta + hls	13 x 4 weeks x 10 min x (100 random faults + 1 reference)	4+3+1+2=10	5.29e6
Heat pump & chiller	COP drop	13 x 4 weeks x 10 min x (100 random faults + 1 reference)	4+7+1+0=12	5.29e6
Solar thermal	Opacification	1 week x 10 min x (14 locations x 5 random faults+1 reference)	4+1+1+5=11	7.1e5
	Hydraulic unbalance	1 week x 5 min x (5 locations x 5 random faults+1 reference)	4+1+1+5=11	5.0e5
Network (pipe, valves & pump)	Leaks	1 week x 5 min x (9 locations x 20 random faults + 1 reference)	4+20+1+9=34	3.7e5
	Excessive Heat Loss	1 week x10 min x(9 locations x 20 random faults + 1 reference)	4+20+1+9=34	1.8e5
Substations	Heat Exchanger Fouling	13 x 4 weeks x 10 min x (100 random faults + 1 ref)	4+3+1+2=10	5.29e6
Hot water storage	Excessive heat Loss	13 x 4 weeks x 10 min x (100 random faults + 1 ref)	4+16+1+0=21	5.29e6

2.4 Evaluation of Machine Learning for FDD

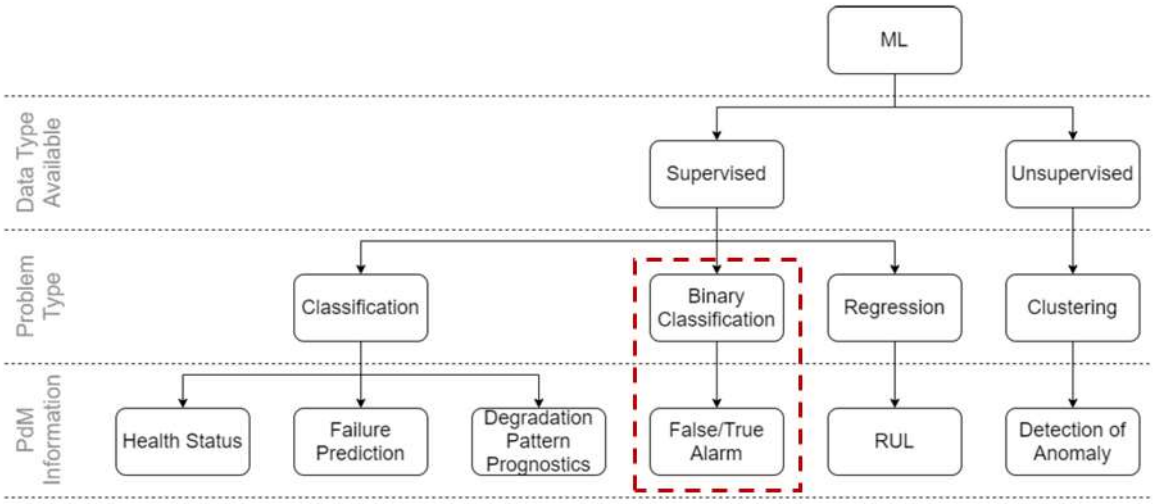

Figure 6 - Possible use of ML models for FDD and focus on the work presented in this paper (adapted from (Olesen and Shaker 2020))

Figure 6 reproduces an overview of possible use of ML models for FDD and predictive maintenance tasks. In this paper, we focus on five supervised binary classification tasks, in which the model should distinguish between two cases (fault / no fault). Table 3 describes these tasks. It should be noted that the generated dataset is also suitable for multi-class classification, leading not only to fault detection but also fault diagnosis. In particular, we can consider two type of multi-class classification cases: fault identification cases, in which several fault can occur and should be distinguished, fault localization cases, in which a fault can occur at different location in the system. Table 4 describes some of the possible multi-class classification tasks. However, presenting these cases is out of scope of this paper: each case would require a more detailed presentation and analysis of the results, and will be presented in upcoming publications.

Table 3 - Cases considered for fault detection using binary classification in this paper

Case ID	Component	Description of the fault
boi_eta	Boiler & CHP	Global reduction of the efficiency of the boiler, which can have several causes (bad combustion, fouling)
boi_hls	Boiler & CHP	Excessive heat losses
hp_cop	HeatPump	COP drop
sst_flg	Substation	Fouling of the substation's heat exchanger
sto_ins	Storage	Degradation of the storage insulation

Table 4 - Possible Fault Diagnosis cases using multi-class classification

Case ID	Component	Description of the fault
boi_multi	**Boiler & CHP**	Possibility to have either a reduction of the combustion efficiency (fault “eta”) or excessive heat losses (fault “hls”) or both at the same time.
sol_unb	**Solar Field**	Hydraulic unbalance of the solar field, which can be attributed to one of the lines (localization)
sol_opa	**Solar Field**	Opacification of panels in the solar field, which can be attributed to one single panel (localization)
net_leaks	**Network**	Localization of leaks in one pipe section of the network
net_hls	**Network**	Localization of excessive heat losses in one pipe section of the network

2.4.1 Data selection

In order to ensure a consistent evaluation on all the binary classification cases, we designed the evaluation as follows:

- All considered data is taken during the heating season (i.e., with boundary conditions corresponding to 4-week period in January – April).

- The train set usually contains 100 time series, randomly chosen from the input dataset. In most cases, since we consider time series with a duration of 4 weeks and sampling of 10 minutes, this typically amounts to 403 200 samples in the train set.

- The test set usually contains 10 time series randomly chosen from the input dataset, **with different boundary conditions than the train set**. The choice of different boundary conditions reflect what would happen in a real setting, where a model would be trained on historical data, and used with new data, whose boundary conditions (weather, demand) will always be different from the training set.

To ensure a good representability of the chosen data despite the relatively small number of time series considered, we tuned the random selection process of the time series to ensure that the obtained distribution is close to the global distribution of

generated faults. As an example, Figure 7 (top) presents the distribution of the characteristics of a set of time series for training, which are the following:

- **Boundary conditions ID**: choice of the boundary condition time series. Here we chose to select as much experiments based on the boundary conditions 1 to 4 (corresponding to weeks 5 to 16 in the year, from the end of January to the end of April).

- **Fault start time**: start time of the fault during the week, in hours. The start time follows a uniform distribution, although in the depicted case there is some bias towards faults starting in the first 2 days.

- **Fault final intensity**: the final intensity of the imposed fault is distributed between 0 and 1, with a truncated half Gaussian distribution, so that there are more cases with small final intensity (minor faults) than cases with high final value (severe faults)

Figure 7 (bottom) presents the distribution of characteristics for a testing set, in which we chose to select only data with boundary conditions corresponding to the beginning of January. We also chose to have a greater number of severe faults in the test set, to ensure that the models can correctly detect them although they are less represented in the training set.

Because of the uniform distribution of start time, the train set is relatively well balanced, with nearly as much samples with/without faults. Samples without faults are a bit more represented, since the dataset also contains reference simulations without faults. On the contrary, the test set contains slightly more samples with faults.

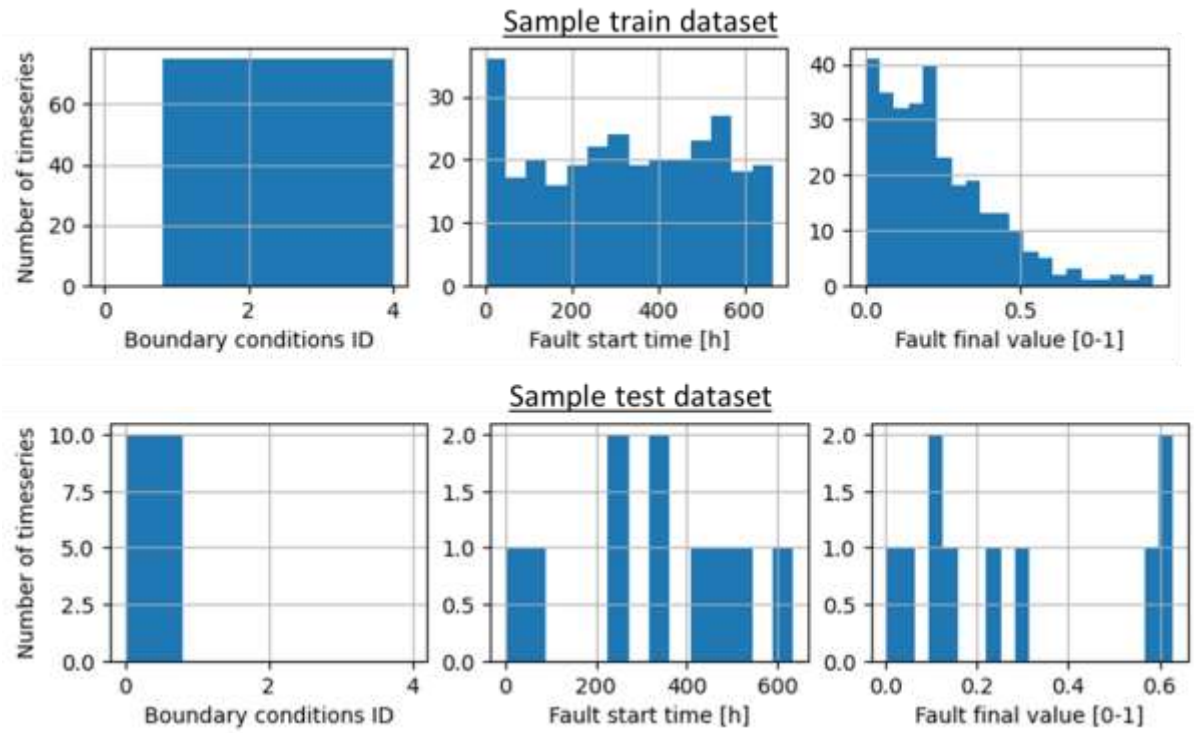

Figure 7 - Example of the distribution of characteristics for 100 time series used for training (top), and 10 time series used for testing (bottom)

2.4.2 Machine-Learning models

Among the great variety of ML models, we considered the models listed in Table 5, as they have been used previous literature on FDD for DHC.

Table 5 - List of Machine Learning models considered in this study

Model ID	Model Name	Used in previous work
LR	Logistic Regresion	[4], [33]
RF	Random Forest	[4], [33]
KNN	K Nearest Neighbors	[33]
SVC	Support Vector Classifier	[33], [45],
XGB	eXtreme-Gradient Boosting	[24], [33], [45]

For each of the models, we performed an optimisation of hyper-parameters using the scikitlearn-hyperopt package [46]. We also included the choice of pre-processing during the optimisation.

2.4.3 Evaluation metrics

Similarly to [33], we considered two main evaluation metrics for this study. The accuracy score is a metric used in most ML applications. The Matthew Correlation Coefficient (MCC) is often used in FDD applications to deal with dataset inbalance and reduce the false positive rate (false alarms). The formulas for accuracy score and MCC are given in equations (1.) and (2.) respectively, where TP stands for True Positive, TN for True Negative, FP for False Positive, FN for False Negative.

Eq 1.: $$Accuracy\ score = \frac{TP+TN}{TP+FP+TN+FN}$$

Eq 2.: $$MCC = \frac{TP \cdot TN - FP \cdot FN}{\sqrt{(TP+FP) \cdot (TP+FN) \cdot (TN+FP) \cdot (TN+FN)}}$$

3 RESULTS

3.1 Binary classification results and comparison

Figure 8 and Figure 9 present the obtained results on the accuracy and MCC criteria, respectively, on the test dataset.

The main insights from these results are the following:

- The results are most of the time similar with both evaluation metrics. This is expected, since our datasets have been designed to be relatively well balanced in terms of the number of records with a fault and without faults.

- Three of the binary classification cases are relatively easy to handle for most Machine-Learning models. For the boiler efficiency fault, the accuracy is over 90% and sometimes close to 100%. For the heat pump COP fault and substation fouling fault, the accuracy is over 85%.

    - On the heat pump COP fault, the poor performance of the KNN model was reproduced several times on the chosen train set, but a different performance was observed with other train sets. This denotes a strong sensitivity of this approach to the chosen data.

- Two of the binary classification cases are more difficult to handle, and both of them are related to heat losses. We identify 2 reasons for these results:

    - The first reason is that this comparative study is based on the raw data from instantaneous records, while effects of heat losses usually take places over longer time periods.

    - The second one is that faults related to heat losses need to be very strong to be detectable in the data, even by a human operator, because they are strongly dependent on the boundary conditions.

Despite these conclusions, we can notice that some models perform better on this type of faults, namely the LR, SVM and XGB models. In fact, this is the case only for the

excessive heat loss fault on the boiler, for which these models obtain higher scores when the fault is both abrupt and intense. The other two models, RF and KNN, provide random predictions independently of the characteristics of the fault.

In the case of the fault on storage insulation, the scores obtained by on the models are also based on random guess, as indicated by a very low MCC score. Only the XGBoost model seem to obtain a higher score. In details, this model tends to predict a fault more often at the end of a simulation run than at the beginning, which provides better scores since the fault probability is 0 at the beginning of a simulation and close to 1 at the end in our simulation setup. Although all models perform prediction on separate instants considered independently without any explicit time information, a correlation with time exits in the boundary conditions (esp. external temperature), which the XGBoost model could pick up to artificially increase its score.

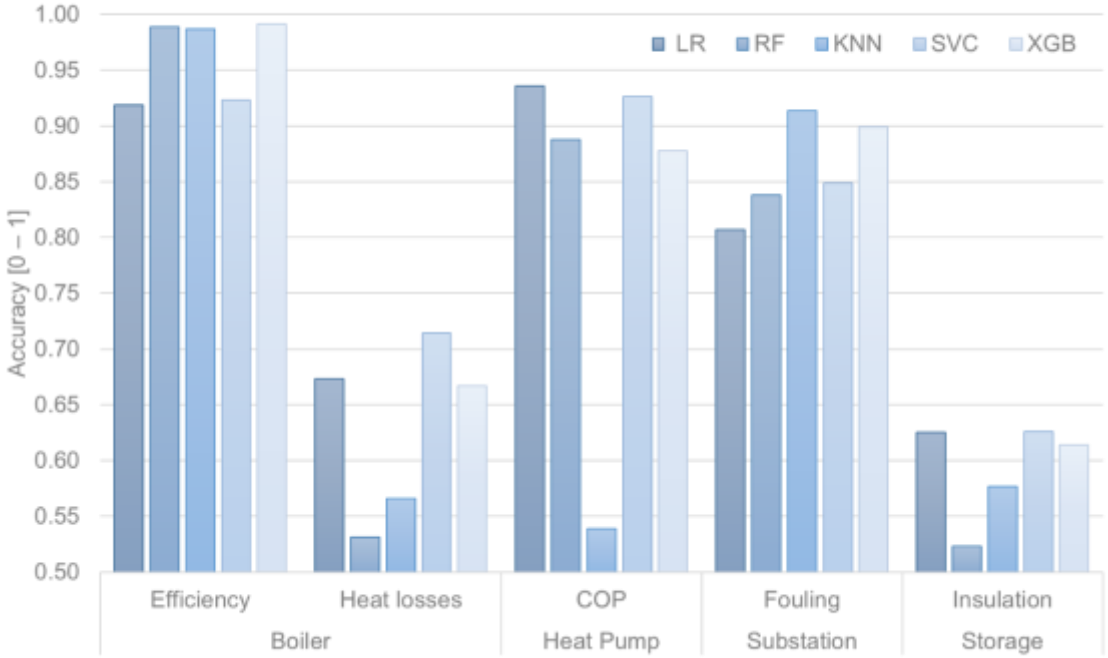

Figure 8 - Accuracy score on the test dataset for each of the evaluated ML model, on the five binary classification cases. The minimum accuracy of 0.5 would amount to a random guess.

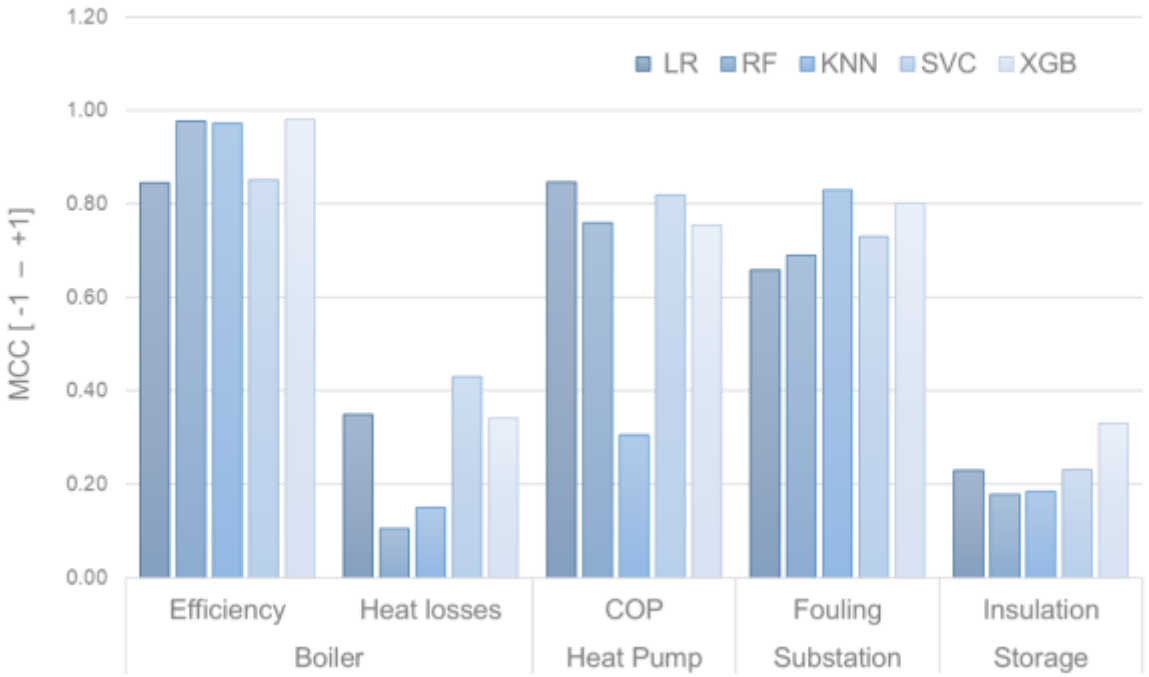

Figure 9 - MCC score on the test dataset for each of the evaluated ML model on the five binary classification cases. A MCC of 0 would correspond to a random guess, and negative values would highlight a tendency to make false predictions even in the case of an imbalanced dataset.

Figure 10 provides a more detailed presentation of the results in the case of applying the LR model for the detection in the heat pump COP drop case. Four difference test cases are provided, with decreasing fault intensities. Both progressive and abrupt faults are considered (as explained in Figure 4), and the indicated percentage refers to the fault intensity at the end of the sequence (100% meaning COP drops to 0).The raw fault detection probabilities are depicted on the left side, and the final predictions are depicted on the right side. Final predictions are obtained by applying a threshold to the probabilities (here 0.5) and filtering out isolated events using a rolling windows averaging (here 24h). The results show that the model can correctly detect even small and progressive anomalies after a few days, while strongly avoiding false alarms. By considering the raw fault detection probabilities, we can also observe that they accurately correlate with the actual fault intensity, especially when the fault appearance is progressive. In the case of a sudden fault (second line), the raw probability immediately jumps to 1, but the final prediction lags by a few hour because of the applied filtering.

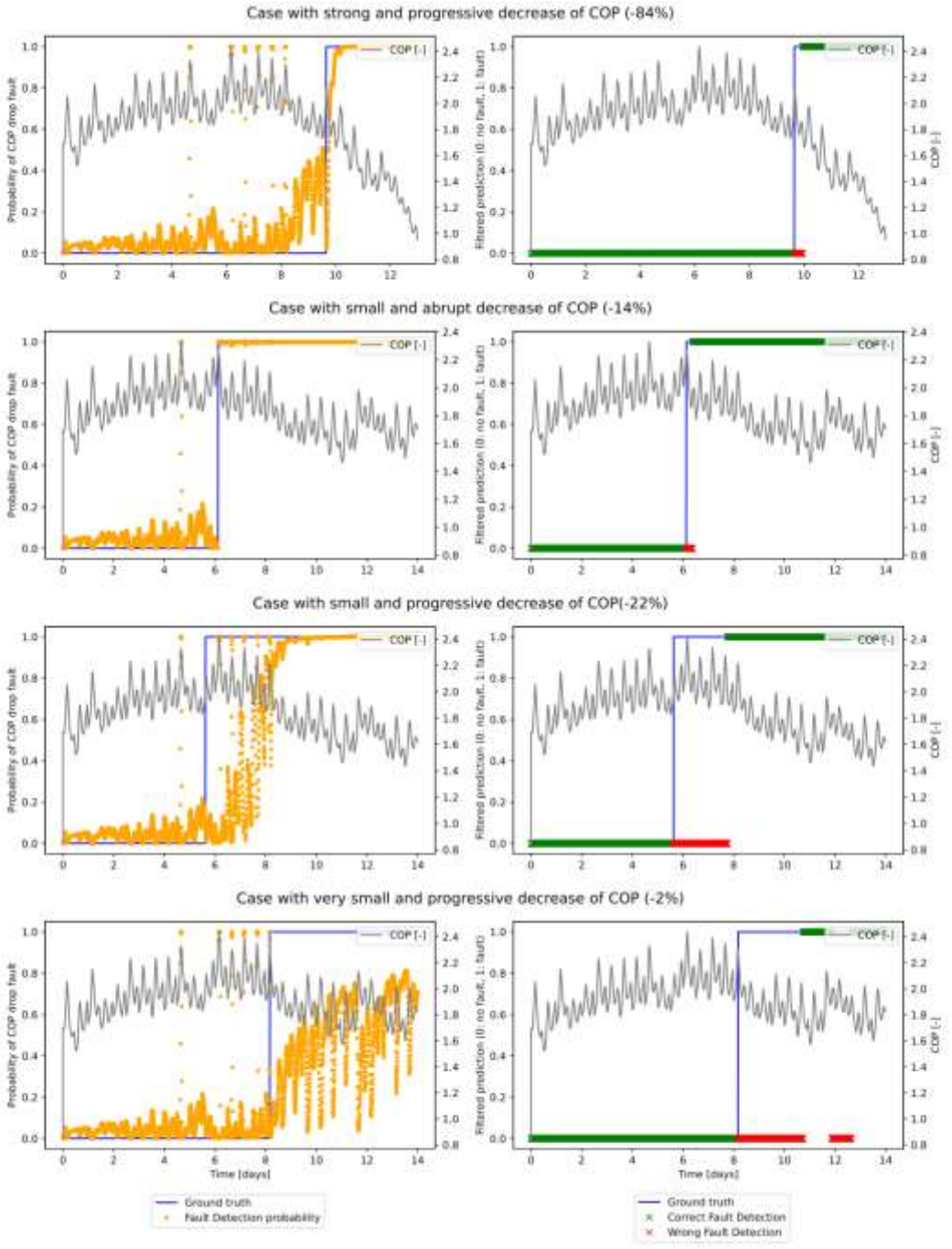

Figure 10 - Detailed results on 4 test cases for the heatpump COP drop case (left: fault detection probability, right: correct and inccorect fault detections after filtering). The grey line indicates the actual value of COP, which is not provided as input to the ML model.

3.2 Ability to transfer a trained models to a different system

In order to assess the ability to use a trained model with an unknown dataset from a different system, the following experiment was performed:

1. Generation of an alternative dataset for a different boiler (boiler B), with a different efficiency curve (see Figure 11, left).

2. Training of a model using i) data containing faults from the previously simulated boiler (source boiler A) and ii) data without faults from the newly generated boiler (target boiler B). This corresponds to the situation where we would have data without faults from the history of a real boiler, and try to detect faults on this boiler although no faulty data is present in the dataset.

3. Test of the model on data containing faults for the target boiler B.

In this experiment, the nominal power and boundary conditions are similar in the previously simulated (source) and newly simulated (target) boiler. This would be consistent with a real use case, in which one would use the historical boundary conditions from a real boiler and apply it to a simulated one to produce faulty data. We also make the hypothesis that the historical data would not contain faults, and we include it in the training set as a reference. On the contrary, the faulty data present in the test set is different both from the faulty data (coming from boiler A) and from the non-faulty data (coming from boiler B) in the train set. In a real setting, this test data would however not be available until a failure occurs on the real system, is detected and is properly labeled.

Figure 11 (left) displays the results obtained for 2 ML classifiers. Although the performance of the models decreases when applied to the target boiler, the MCC score remains relatively high and denotes both a correct detection of faults and a relatively low number of false alarms.

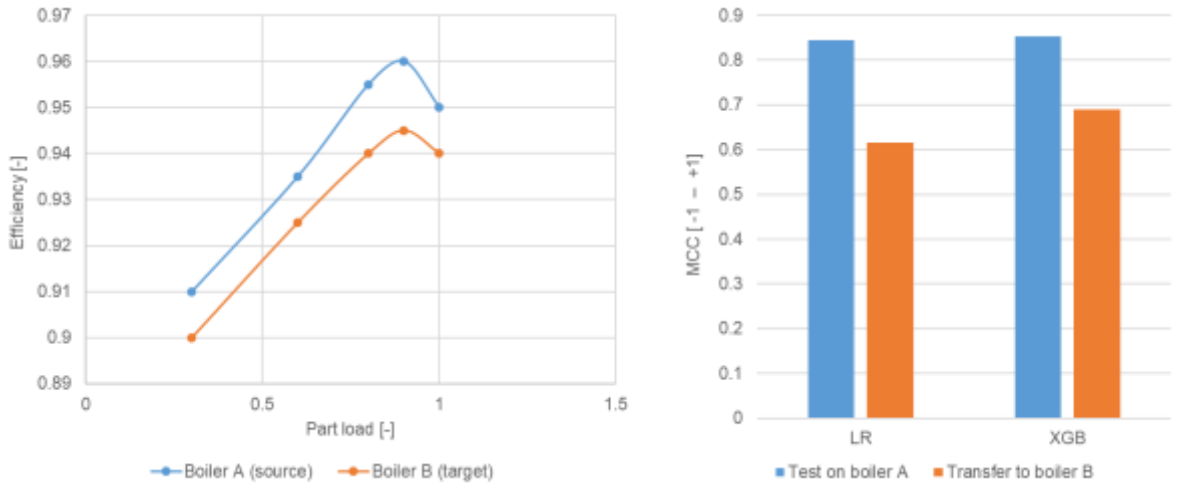

Figure 11 - Efficiency curves (left) and fault detection results (right) when applying a model trained on a source boiler (A) to a target boiler (B)

3.3 Application to a real-world data

Despite the lack of openly available data from real-world systems, we could at least assess the performance of a trained model on the simulated dataset on the substation fouling case, using data available on a Kaggle repository [47]. Since this dataset does not contain fault annotations, we assumed that no fault was present.

Figure 12 presents the results of testing the model trained on the simulated substation dataset on the real substation data. While the trained model sometimes detects anomalies, these events are always punctual. Considering that an alert is triggered only after 1h of consistent anomaly detection eliminates any false alarm. Figure 12 also depicts the variation of an estimation of the heat exchanger (HEX) overall conductance (UA) obtained using the classical LMTD formula [48]. It is interesting to notice that although the HEX conductance varies significantly during the year, the model correctly classifies the situation as non-faulty.

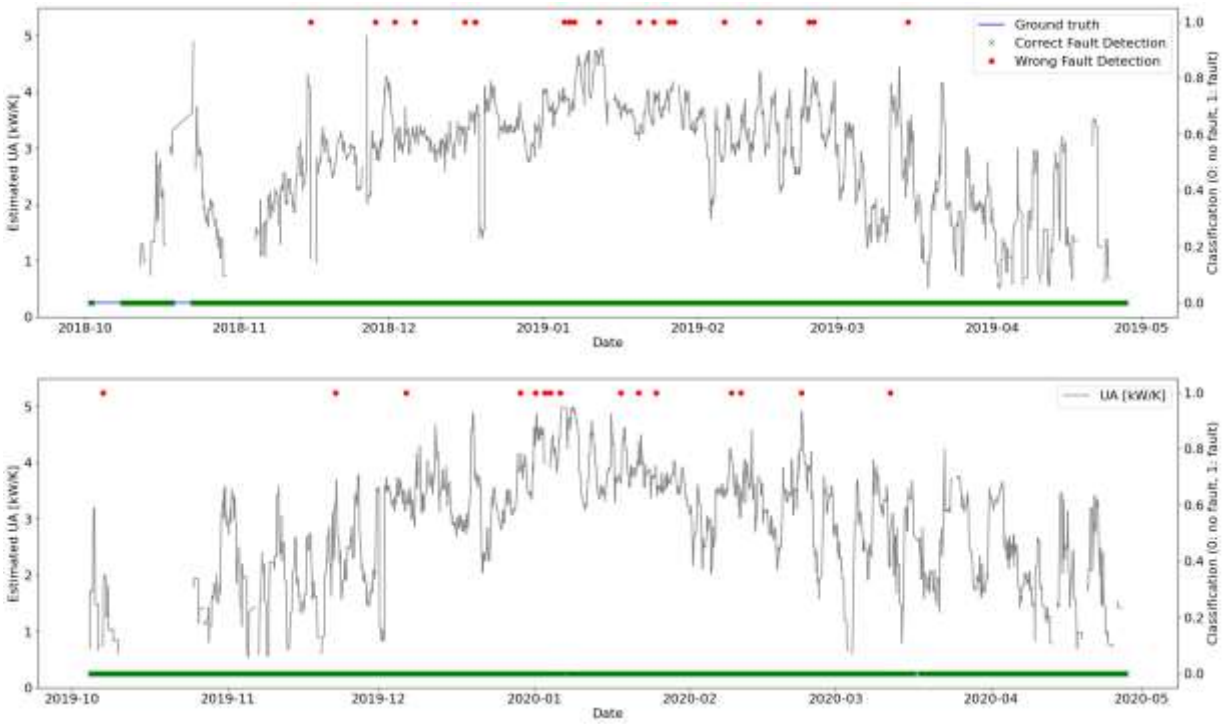

Figure 12 - Test of a fault detection model on real-world data (without faults). The heat exchanger conductivity UA is estimated from the data using the classical LMTD formula.

4 CONCLUSION AND PERSPECTIVES

In this work, we investigate the possibility for DHC operators to detect and diagnose faults in a DHC system under the assumptions that (i) no specific sensors need to be installed, (ii) datasets do not have to contain previous examples of faults with correct annotations.

To this aim, we use simulation to create a synthetic dataset for several types of faults which can occur in DHC system production, distribution or storage components. This dataset is provided as Open Data in order to serve as a reference for future research.

After presenting the generation of the synthetic fault dataset, we evaluate the performance of Machine Learning (ML) models on five fault detection tasks. The results highlight varying level of performance among the considered tasks, with faults related to global energy efficiency being easier to handle than those related specifically to thermal losses. Although this initial result can be improved with more refined ML models, it reveals the difficulty to detect faults related to thermal losses, which are often strongly dependent on the boundary conditions. As a consequence, this type of faults should probably be investigated in practice with a combination of Machine Learning and other methods such as infrared thermography.

We also observe that three of the investigated models (Logistic Regression, Support Vector Machine, and XGBoost) provide consistent performance on the considered tasks, achieving accuracy scores up to 99% on the easier tasks and above 66% on one of the more difficult tasks.

In addition, we illustrate the possibility to transfer the results to a different system,with encouraging results. Although the performance may be reduced, we obtain consistent results when applying a model trained on our dataset to data produced either by another simulation model or by a real system. More advanced transfer learning techniques, especially using Deep Learning methods, could be investigated to confirm these results.

Future works will cover additional experiments with the dataset, especially considering multi-class classification. Combination with other data from real-world system should also be attempted, depending on the availability of such data.

ACKNOWLEDGMENTS

This work was financially supported by the IEA DHC Annex XIII program, in the frame of the project “AI for Forecasting and Fault Detection in DHN” (contract n° XIII-3)
https://www.iea-dhc.org/the-research/annexes/annex-xiii/annex-xiii-project-03

DATA AVAILABILITY

Datasets and models related to this article can be found at
https://www.kaggle.com/datasets/mathieuvallee/ai-dhc and
https://github.com/mathieu-vallee/ai-dhc

REFERENCES

[1] Euroheat&Power, “Digital Roadmap for District Heating and Cooling,” May 2018. Accessed: Feb. 28, 2019. [Online]. Available: https://www.euroheat.org/publications/digital-roadmap-district-heating-cooling/
[2] E. O’Dwyer, I. Pan, S. Acha, and N. Shah, “Smart energy systems for sustainable smart cities: Current developments, trends and future directions,” *Applied Energy*, vol. 237, pp. 581–597, Mar. 2019, doi: 10.1016/j.apenergy.2019.01.024.
[3] G. Mbiydzenyuy, S. Nowaczyk, H. Knutsson, D. Vanhoudt, J. Brage, and E. Calikus, “Opportunities for Machine Learning in District Heating,” *Applied Sciences*, vol. 11, no. 13, Art. no. 13, Jan. 2021, doi: 10.3390/app11136112.
[4] C. Ntakolia, A. Anagnostis, S. Moustakidis, and N. Karcanias, “Machine learning applied on the district heating and cooling sector: a review,” *Energy Systems*, vol. 13, no. 1, 2022, doi: 10.1007/s12667-020-00405-9.
[5] S. Katipamula and M. Brambley, “Review Article: Methods for Fault Detection, Diagnostics, and Prognostics for Building Systems—A Review, Part I,” *HVAC&R Res.*, vol. 11, no. 1, pp. 3–25, Jan. 2005, doi: 10.1080/10789669.2005.10391123.
[6] V. Venkatasubramanian, R. Rengaswamy, K. Yin, and S. N. Kavuri, “A review of process fault detection and diagnosis: Part I: Quantitative model-based methods,” *Computers & Chemical Engineering*, vol. 27, no. 3, pp. 293–311, Mar. 2003, doi: 10.1016/S0098-1354(02)00160-6.
[7] J. Granderson, R. Singla, E. Mayhorn, P. Ehrlich, D. Vrabie, and S. Frank, “Characterization and Survey of Automated Fault Detection and Diagnostic Tools,” Lawrence Berkeley National Laboratory, LBNL-2001075, 2017. [Online]. Available: https://flexlab.lbl.gov/publications/characterization-and-survey-automated
[8] G. Faure, M. Vallée, C. Paulus, and T. Q. Tran, “Fault detection and diagnosis for large solar thermal systems: A review of fault types and applicable methods,” *Solar Energy*, vol. 197, pp. 472–484, Feb. 2020, doi: 10.1016/j.solener.2020.01.027.
[9] J. F. Olesen and H. R. Shaker, “Predictive Maintenance for Pump Systems and Thermal Power Plants: State-of-the-Art Review, Trends and Challenges,” *Sensors*, vol. 20, no. 8, Art. no. 8, Jan. 2020, doi: 10.3390/s20082425.
[10] S. Buffa, M. H. Fouladfar, G. Franchini, I. Lozano Gabarre, and M. Andrés Chicote, “Advanced Control and Fault Detection Strategies for District Heating and Cooling Systems—A Review,” *Applied Sciences*, vol. 11, no. 1, Art. no. 1, Jan. 2021, doi: 10.3390/app11010455.
[11] R. Isermann, *Fault-Diagnosis Systems - An Introduction from Fault Detection to Fault Tolerance*. 2006. Accessed: Dec. 05, 2014. [Online]. Available: http://www.springer.com/engineering/control/book/978-3-540-24112-6
[12] M. Vallee, N. Lamaison, and T. Wissocq, “Report on Fault Data and Fault Simulation Models for Components of a DHC system,” 2022.
[13] X. Yang, Q. Zhao, Y. Wang, and K. Cheng, “Fault signal reconstruction for multi-sensors in gas turbine control systems based on prior knowledge from time series representation,” *Energy*, vol. 262, p. 124996, Jan. 2023, doi: 10.1016/j.energy.2022.124996.
[14] Y. Park, M. Choi, and G. Choi, “Fault detection of industrial large-scale gas turbine for fuel distribution characteristics in start-up procedure using artificial neural network method,” *Energy*, vol. 251, p. 123877, Jul. 2022, doi: 10.1016/j.energy.2022.123877.

[15] R. Panday, N. Indrawan, L. J. Shadle, and R. W. Vesel, “Leak detection in a subcritical boiler,” *Applied Thermal Engineering*, vol. 185, p. 116371, Feb. 2021, doi: 10.1016/j.applthermaleng.2020.116371.
[16] P. Hundi and R. Shahsavari, “Comparative studies among machine learning models for performance estimation and health monitoring of thermal power plants,” *Applied Energy*, vol. 265, p. 114775, May 2020, doi: 10.1016/j.apenergy.2020.114775.
[17] IEA EBC Annex 25, “Building Optimization and Fault Diagnosis Source Book,” Aug. 1996.
[18] M. Kim, W. V. Payne, P. A. Domanski, S. H. Yoon, and C. J. L. Hermes, “Performance of a residential heat pump operating in the cooling mode with single faults imposed,” *Applied Thermal Engineering*, vol. 29, no. 4, pp. 770–778, Mar. 2009, doi: 10.1016/j.applthermaleng.2008.04.009.
[19] B. Cai *et al.*, “Multi-source information fusion based fault diagnosis of ground-source heat pump using Bayesian network,” *Applied Energy*, vol. 114, pp. 1–9, Feb. 2014, doi: 10.1016/j.apenergy.2013.09.043.
[20] W. Nelson and C. Culp, “Machine Learning Methods for Automated Fault Detection and Diagnostics in Building Systems—A Review,” *Energies*, vol. 15, no. 15, Art. no. 15, Jan. 2022, doi: 10.3390/en15155534.
[21] S. P. Melgaard, K. H. Andersen, A. Marszal-Pomianowska, R. L. Jensen, and P. K. Heiselberg, “Fault Detection and Diagnosis Encyclopedia for Building Systems: A Systematic Review,” *Energies*, vol. 15, no. 12, Art. no. 12, Jan. 2022, doi: 10.3390/en15124366.
[22] G. Li, L. Chen, J. Liu, and X. Fang, “Comparative study on deep transfer learning strategies for cross-system and cross-operation-condition building energy systems fault diagnosis,” *Energy*, vol. 263, p. 125943, Jan. 2023, doi: 10.1016/j.energy.2022.125943.
[23] X. Zhu, K. Chen, B. Anduv, X. Jin, and Z. Du, “Transfer learning based methodology for migration and application of fault detection and diagnosis between building chillers for improving energy efficiency,” *Building and Environment*, vol. 200, p. 107957, Aug. 2021, doi: 10.1016/j.buildenv.2021.107957.
[24] P. Xue, Y. Jiang, Z. Zhou, X. Chen, X. Fang, and J. Liu, “Machine learning-based leakage fault detection for district heating networks,” *Energy and Buildings*, vol. 223, p. 110161, Sep. 2020, doi: 10.1016/j.enbuild.2020.110161.
[25] L. Manservigi, H. Bahlawan, E. Losi, M. Morini, P. R. Spina, and M. Venturini, “A diagnostic approach for fault detection and identification in district heating networks,” *Energy*, vol. 251, p. 123988, Jul. 2022, doi: 10.1016/j.energy.2022.123988.
[26] H. Bahlawan *et al.*, “Detection and identification of faults in a District Heating Network,” *Energy Conversion and Management*, vol. 266, 2022, doi: 10.1016/j.enconman.2022.115837.
[27] H. Gadd and S. Werner, “Fault detection in district heating substations,” *Applied Energy*, vol. 157, pp. 51–59, Nov. 2015, doi: 10.1016/j.apenergy.2015.07.061.
[28] S. Månsson, P.-O. Johansson Kallioniemi, M. Thern, T. Van Oevelen, and K. Sernhed, “Faults in district heating customer installations and ways to approach them: Experiences from Swedish utilities,” *Energy*, vol. 180, pp. 163–174, Aug. 2019, doi: 10.1016/j.energy.2019.04.220.
[29] P. Leoni, R. Geyer, and R.-R. Schmidt, “Developing innovative business models for reducing return temperatures in district heating systems: Approach and first

results," *Energy*, vol. 195, p. 116963, Mar. 2020, doi: 10.1016/j.energy.2020.116963.
[30] A. Fabre, "Développement d'indicateurs de performance et de détection de défauts sur les réseaux de chaleur dans une démarche d'optimisation de leur pilotage," These de doctorat, Université Paris sciences et lettres, 2020. Accessed: Jul. 01, 2022. [Online]. Available: http://theses.fr/fr/2020UPSLM077
[31] R. Kim, Y. Hong, Y. Choi, and S. Yoon, "System-level fouling detection of district heating substations using virtual-sensor-assisted building automation system," *Energy*, vol. 227, p. 120515, Jul. 2021, doi: 10.1016/j.energy.2021.120515.
[32] J. Granderson, G. Lin, A. Harding, P. Im, and Y. Chen, "Building fault detection data to aid diagnostic algorithm creation and performance testing," *Sci Data*, vol. 7, no. 1, Art. no. 1, Feb. 2020, doi: 10.1038/s41597-020-0398-6.
[33] G. Bode, S. Thul, M. Baranski, and D. Müller, "Real-world application of machine-learning-based fault detection trained with experimental data," *Energy*, vol. 198, p. 117323, May 2020, doi: 10.1016/j.energy.2020.117323.
[34] L. von Rueden *et al.*, "Informed Machine Learning - A Taxonomy and Survey of Integrating Prior Knowledge into Learning Systems," *IEEE Transactions on Knowledge and Data Engineering*, pp. 1–1, 2021, doi: 10.1109/TKDE.2021.3079836.
[35] J. Willard, X. Jia, S. Xu, M. Steinbach, and V. Kumar, "Integrating Scientific Knowledge with Machine Learning for Engineering and Environmental Systems," *ACM Comput. Surv.*, vol. 55, no. 4, p. 66:1–66:37, Nov. 2022, doi: 10.1145/3514228.
[36] P. Westermann, M. Welzel, and R. Evins, "Using a deep temporal convolutional network as a building energy surrogate model that spans multiple climate zones," *Applied Energy*, vol. 278, p. 115563, Nov. 2020, doi: 10.1016/j.apenergy.2020.115563.
[37] A. T. D. Perera, P. U. Wickramasinghe, V. M. Nik, and J.-L. Scartezzini, "Machine learning methods to assist energy system optimization," *Applied Energy*, vol. 243, pp. 191–205, Jun. 2019, doi: 10.1016/j.apenergy.2019.03.202.
[38] J. J. Downs and E. F. Vogel, "A plant-wide industrial process control problem," *Computers & Chemical Engineering*, vol. 17, no. 3, pp. 245–255, Mar. 1993, doi: 10.1016/0098-1354(93)80018-I.
[39] C. A. Rieth, B. D. Amsel, R. Tran, and M. B. Cook, "Additional Tennessee Eastman Process Simulation Data for Anomaly Detection Evaluation." Harvard Dataverse, 2017. doi: 10.7910/DVN/6C3JR1.
[40] A. Lavin *et al.*, "Technology readiness levels for machine learning systems," *Nat Commun*, vol. 13, no. 1, Art. no. 1, Oct. 2022, doi: 10.1038/s41467-022-33128-9.
[41] G. Faure, M. Vallée, C. Paulus, and T. Q. Tran, "Impact of faults on the efficiency curve of flat plate solar collectors: a numerical analysis," *Journal of Cleaner Production*, vol. 231, pp. 794–804, Sep. 2019, doi: 10.1016/j.jclepro.2019.05.122.
[42] D. Müller, M. R. Lauster, A. Constantin, M. Fuchs, and P. Remmen, "AixLib - An Open-Source Modelica Library within the IEA-EBC Annex60 Framework," presented at the BauSIM 2016, Stuttgart: Fraunhofer IRB Verlag, 2016.
[43] M. Vallee, *mathieu-vallee/ai-dhc*. 2022. [Online]. Available: https://github.com/mathieu-vallee/ai-dhc
[44] M. Vallee, "[dataset] Fault Detection and Diagnosis in District Heating," Dec. 20, 2022. https://www.kaggle.com/datasets/mathieuvallee/ai-dhc
[45] J. Chen, L. Zhang, Y. Li, Y. Shi, X. Gao, and Y. Hu, "A review of computing-based automated fault detection and diagnosis of heating, ventilation and air conditioning

systems," *Renewable and Sustainable Energy Reviews*, vol. 161, p. 112395, Jun. 2022, doi: 10.1016/j.rser.2022.112395.
[46] B. Komer, J. Bergstra, and C. Eliasmith, "Hyperopt-Sklearn: Automatic Hyperparameter Configuration for Scikit-Learn," presented at the Python in Science Conference, Austin, Texas, 2014, pp. 32–37. doi: 10.25080/Majora-14bd3278-006.
[47] M. Zdrakovic, "Towards XAI-assisted DHS operations," 2020. https://kaggle.com/code/milanzdravkovic/towards-xai-assisted-dhs-operations (accessed Dec. 20, 2022).
[48] "Logarithmic mean temperature difference," *Wikipedia*. Apr. 07, 2023. Accessed: Apr. 16, 2023. [Online]. Available: https://en.wikipedia.org/w/index.php?title=Logarithmic_mean_temperature_difference&oldid=1148587120